GEOPHYSICS, VOL. 64, NO. 2 (MARCH-APRIL 1999); P. 368–377, 8 FIGS.

Case History

Seismic attributes for monitoring of a shallow heated heavy oil reservoir: A case study

Douglas R. Schmitt*

ABSTRACT

In production geophysics, detecting the zones of production or constraining the in-situ conditions within a reservoir are often of greater importance than obtaining highly resolved seismic structural images. Standard seismic data processing distorts the signal and limits the potential for extracting additional information, especially for shallow targets. An alternative "shift-stack" procedure is applied in the processing of a shallow 12-fold, 1-m common midpoint (CMP) spacing reflection profile acquired over a heated Athabasca heavy oil sand reservoir. The shift-stack involves summing of CMP traces which have been flattened to an appropriate reference event. Simple modeling confirms that the prestack waveforms are better preserved by this process. Amplitude and frequency attributes are extracted from the reflection profile. Amplitudes of a continuous reservoir event vary by 600% over 35-m intervals along the profile. Bright spots correlate with heated regions. Apparent frequencies, as measured by the instantaneous frequency and by short time-window power spectral estimates of the subreservoir event are 20–30 Hz lower in these same regions. These diminished apparent frequencies most probably result from interference of the subreservoir reflection with events related to structural changes within the reservoir. A complete interpretation of the results has not been attempted as knowledge of the in-situ conditions is incomplete. However, changes in the seismic response at the well locations suggest that these attributes are useful in detection and mapping of heated zones. The shift-stack procedure may also be useful in environmental and geotechnical applications.

INTRODUCTION

As practiced, the common midpoint (CMP) method relies on a number of approximations that are valid only for short source-receiver offsets. In particular, waveforms corrected by normal moveout (NMO) can be severely distorted if the short offset assumption is violated. These distortions degrade the frequency and amplitude attributes derived from the stacked waveforms. Such a situation is encountered in subtle attribute analyses of shallow developed reservoirs. In these cases, the underlying structure is already well known; locating those portions of the reservoir bypassed by the artificial stimulation is of greater concern. Estimating in-situ physical properties or conditions may also be an important priority in shallow-reservoir seismic profiling. The waveform distortion and the smoothing intrinsic to the CMP-NMO method may eliminate much of the important information within the waveforms necessary to correctly interpret the profile.

In addition to waveform distortions, other effects can influence the quality of shallow reflection profiles. These include interference of desired reflected energy with direct, refracted, surface, and air waves, inconsistencies in source triggering, rapid changes in the near-surface material velocity (e.g., Knapp and Steeples, 1986; Steeples and Miller, 1990), and offset dependent changes in reflection amplitudes (e.g., Pullan and Hunter, 1985).

In this paper, I suggest an alternative approach to the processing of shallow reflection profiles acquired in specific, well-controlled situations. Development of this approach was motivated by the difficulties encountered in conventional processing of CMP data acquired over a shallow heavy oil reservoir into which steam has been injected. In this case, preserving prestack waveforms was much more important than creating a highly resolved image of the relatively featureless flat-lying geology. I find that the magnitudes of amplitude and frequency

Manuscript received by the Editor September 3, 1997; revised manuscript received September 28, 1998.
*Institute of Geophysics, Meteorology and Space Physics, Department of Physics, University of Alberta, Edmonton, Alberta T6G 2J1, Canada. E-mail: doug@phys.ualberta.ca.

attributes show great sensitivity to the changes in material properties at the known positions of the horizontal injecting wells. The interpretation of these attributes remains ambiguous due an incomplete understanding of the variations in the physical properties within the reservoir undergoing steam injection. The attributes in this study will be used in on-going time-lapse seismic studies of the same area employing differential attributes.

GEOLOGY AND SEISMIC CHARACTER

The experiments were carried out in northeastern Alberta at a site where viscous heavy oils are being produced from shallow (120–160-m) bituminous Athabasca oil sands of the Lower Cretaceous McMurray Formation. The geology is described extensively by Wrightman et al. (1989, 1995) and several earlier seismic studies have been carried out in the region (Pullin et al. 1987; Paulsson et al., 1994). Briefly, at this site the McMurray reservoir consists of weakly consolidated fluvial quartz sands with a 30–40% average porosity. The oil sands at this site are composed of 10–18 wt.% bitumen with saturations ranging from 65% to 97%. The viscous bitumen ($\sim$17–20 Pa $\cdot$ s) is recovered with the "steam-assisted gravity drainage" technique (e.g., Butler, 1994; Ali and Thomas, 1996; Chow and Butler, 1996) in which pairs of horizontal wellbores lying near the bottom of the reservoir are used for injection and production. The in-situ velocity of this heavy oil—filled porous sand, as measured by the sonic log prior to steam injection (Figure 1), is approximately 2400 m/s and is relatively constant with depth (Kebaili and Schmitt, 1996).

The McMurray oil sands lie immediately above a thick sequence of competent and high-velocity (>3000 m/s) Paleozoic carbonates (160-m depth) and immediately below the approximately 2.5–3-m thick low velocity ($\approx$1500 m/s) Wabiskaw member (122.5-m depth), a glauconitic sand containing gas and water within the Clearwater formation. Series of layered thin marine silts and shales, some of which are highly competent, compose the overlying Clearwater and Grand Rapids formations. Both the top and bottom reservoir contacts are abrupt erosional unconformities. Along the short profile length in this investigation, these geologic contacts as well as the surface topography are flat lying.

Expected reflection seismic responses modeled from the sonic log velocities (Figure 2) using an ARMA method (e.g., Treitel and Robinson, 1966) indicate the strongest events are returned from the Wabiskaw member (129-ms model time) and from the top of the Paleozoic carbonates (158-ms model time). These are referred to hereafter as the "gas-sand" and the "unconformity" events. These two strong events are useful in seismic monitoring as they are produced by large impedance variations across geologic unconformities bounding the oil sands.

The introduction of heated water into the reservoir changes stress, pore pressure, and temperature. These factors influence the elastic wave velocities (Nur, 1987), but predicting actual material properties is a challenge even if complete knowledge of the competing extrinsic variables is available. Elevated temperatures result in diminished velocities in both the rock matrix (e.g., Timur, 1977) and the reservoir fluids (e.g., Batzle and Wang, 1992; Clark, 1992). Greater compressional stresses make the rock matrix less compressible, thus increasing velocity (e.g., Domenico, 1977). In contrast, elevated pore pressures subject the material to a lower effective confining stress with reduced velocities (e.g., Christensen and Wang, 1985). This last effect is complicated by the exsolution of gas from live oils when pore pressures are reduced. The appearance of gas bubbles results in large changes in overall compressibility. It is further likely that the matrix of these weak materials is permanently deformed, and this disruption is expected to influence the velocity. Shifts in the extrinsic conditions and fluid saturations influence the attenuative properties with the quality factor Q normally increasing with velocity.

Both pore pressure and temperature increases during the recovery process, especially in the vicinity of the injecting wells. Declines in the seismic wave speed as great as 20% can result from these changes in the reservoir conditions. Theoretical predictions (Hickey et al., 1991), ultrasonic laboratory measurements (Wang and Nur, 1990; Eastwood, 1993), push-down effects in reflection profiles (Kalantzis et al., 1993; Eastwood et al., 1994; Lumley, 1995), repeated sonic logs (Siewert, 1994), and high-frequency cross-well tomography (Macrides et al., 1988; Paulsson et al., 1994; Mathisen et al., 1995) all indicate that such changes in velocity are possible.

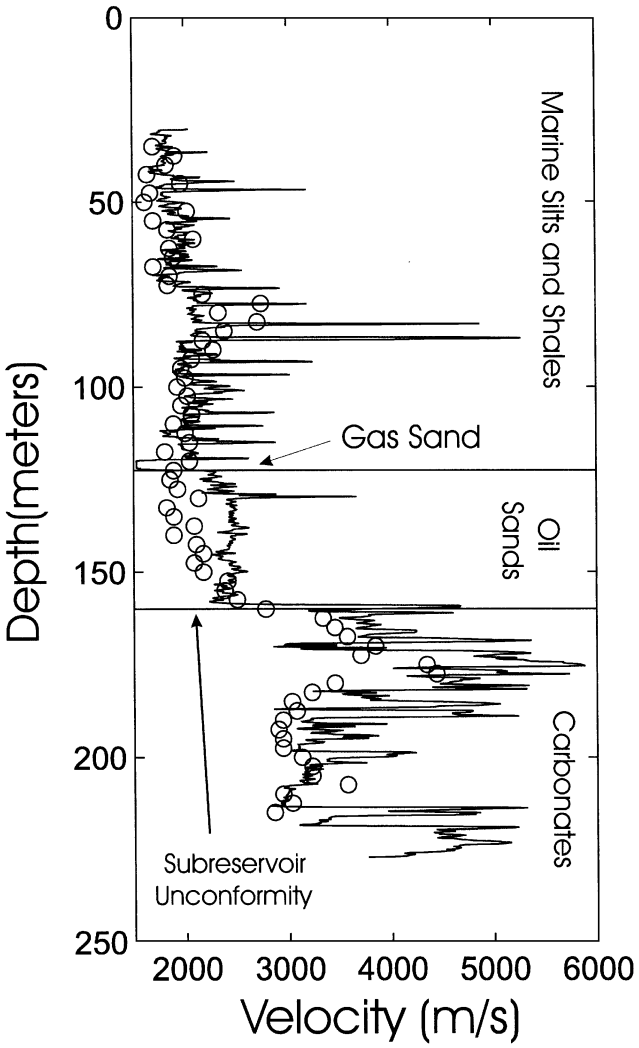

FIG. 1. Characteristic sonic well log velocities (line) and vertical seismic profiling (VSP) interval velocities (open circles) with depth in a vertical well adjacent to the profile.

It remains to be determined whether predicted changes in material properties are detectable by surface seismic methods. A hypothetical velocity structure wherein the compressional wave velocity within the oil sands decreases due to heating from 2400 m/s (Figure 2a) to 2000 m/s (Figure 2d) and with a thermal gradient dependent gradation in velocity at the top of the reservoir suggests that the unconformity reflector would be delayed 6 ms from 158 ms (Figure 2b) to 164 ms (Figure 2c). Further, the peak amplitude of the unconformity event is noticeably greater because of the impedance contrast across the sharp boundary between the carbonates and the oil sands. In summary, the seismic modeling indicates that both traveltimes and amplitudes can be used in monitoring.

FIELD PROCEDURES AND DATA PROCESSING

A 12-fold seismic reflection profile was acquired on a packed road over the reservoir using standard procedures (e.g., Steeples and Miller, 1990). The profile is perpendicular to three pairs of horizontal injecting and producing wellbores lying near the base of the oil sands and referred to as B1, B2, and B3. A wave test was first carried out over the site with an accelerated weight-drop source. A single geophone placed immediately beside the point of impact provided the trigger signal. Strong near-surface refracted air and surface wave arrivals interfered with the desired gas-sand and unconformity events. A source-receiver offset window between 52 and 98 m was finally employed to reduce these unwanted arrivals in a manner similar to the "optimum window" technique of Hunter et al. (1984). The gas-sand and unconformity traveltime curves were determined by ray tracing and the NMO approximation using VSP-derived interval velocities (Figure 1). The traveltime errors of the NMO approximation are negligible over the offset range used. The frequency distortions introduced by the NMO correction, however, are substantial.

In all, ninety-five 24-trace common shot records with 2-m shot and receiver spacings were acquired in an end-on spread

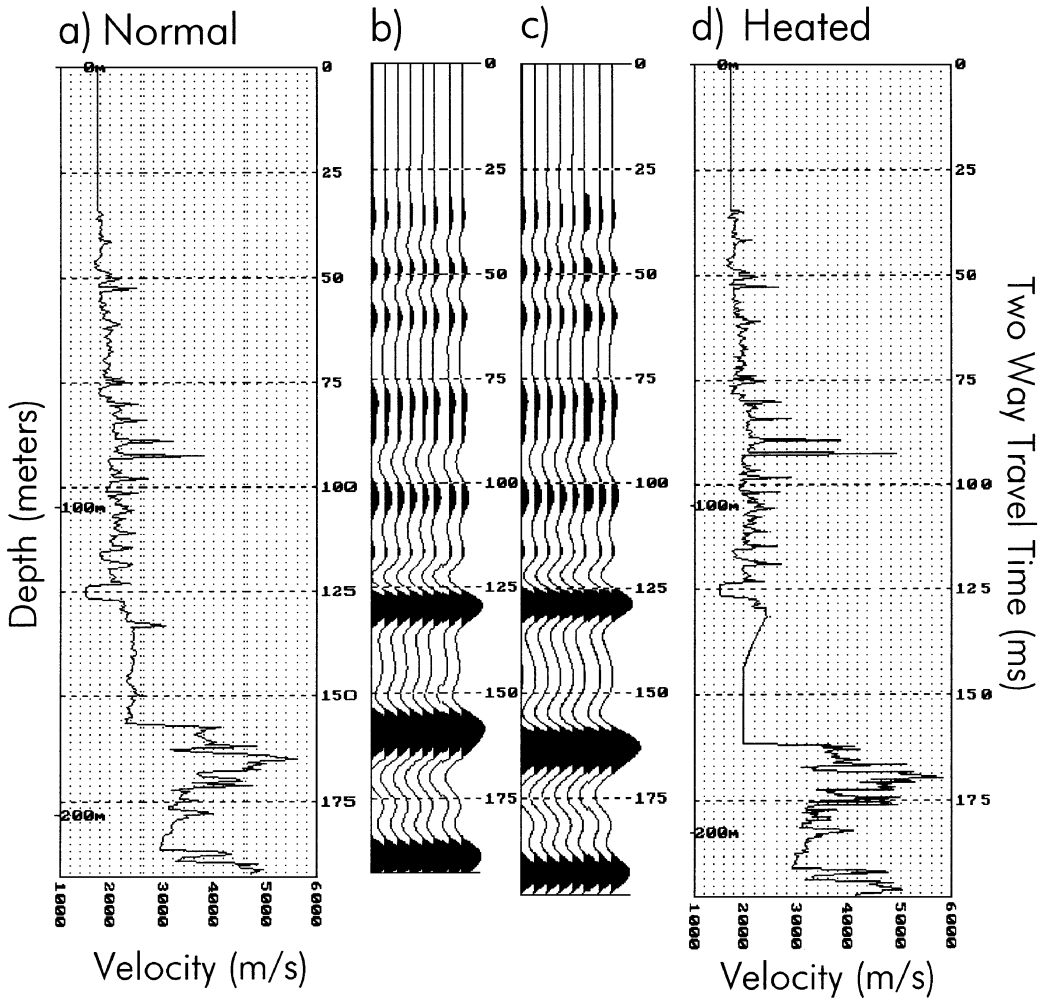

FIG. 2. (a) Observed sonic log velocities versus traveltime prior to heating of the reservoir; (b) 50-Hz Ricker wavelet synthetic seismogram for the preheated reservoir; (c) 50-Hz Ricker wavelet synthetic seismogram for the heated reservoir; and (d) hypothetical sonic log after heating of the reservoir. Two-way model traveltimes are arbitrarily shifted, and these absolute times do not correspond to traveltimes in later figures. Variations in sonic curves are plotting artifacts.

configuration (e.g., Figure 3). This resulted in 212 stacked CMP traces at a 1-m spacing with a 12-fold redundance. Each raw trace is the signal from a string of 4.5-Hz resonant frequency geophones (4.5–200 Hz nominal bandpass) closely planted (within 1 m perpendicular to the profile line) at the corresponding offset station distance. As such, this geophone group acts as a point detector.

Data were acquired with a 0.5-ms sampling interval. Only a high-cut antialias filter with a corner frequency of 500 Hz was employed. This diminished substantially the higher frequency air wave, but retained the low-frequency surface wave.

Positive lobes of the gas-sand and unconformity events appear at approximately 175 ms and 190 ms, respectively, in raw common shot gathers (e.g., Figure 3a). These reflected events have very little moveout across this limited aperture array. In contrast, other arrivals, here considered as noise, have noticeable dips. This contrast in dip was taken advantage of in an f-k filtering strategy. This filtering was carried out by first flattening the traces in the common shot gather according to the moveout of the shallow refractions (about 1700 m/s). This has the advantage that the reflected events have a negative apparent moveout. Consequently, they are distinctly separate in the f-k domain, simplifying removal of those portions with zero or with positive moveout. The result, which also includes a bandpass filter between 8 and 120 Hz, shows particular enhancement of the gas-sand and unconformity events (Figure 3b), although substantial contamination from the shallow refractions remains. These filtered traces are then reorganized into common offset gathers before final processing.

THE SHIFT-STACK

The advantage of CMP-NMO stacking is that random and coherent noise is attenuated relative to the desired reflected signal (Yilmaz, 1987). Traveltimes are transformed to those expected for a hypothetical zero-offset at the source-receiver midpoint. In practice, this time shift is accomplished with the offset-and time-dependent normal moveout correction t:

$$\Delta t = \left\{ \frac{x^2}{v^2} + t_o^2 \right\}^{\frac{1}{2}} - t_o, \tag{1}$$

where t_o is the normal incidence two-way traveltime, x is the source-receiver offset, and v is the stacking velocity. Application of equation (1), or for that matter any more accurate normal moveout correction scheme, is accompanied by an unavoidable time stretch which changes an original frequency f to f' according to

$$f' = f\left(1 + \frac{d(\Delta t)}{dt_o}\right). \tag{2}$$

This frequency distortion is most severe at short times and long offsets (relative to the depth of the reflector) and can degrade the image quality of shallow reflection profiles (Miller, 1992). In deeper seismic exploration, this distorted signal is eliminated in muting. However, in this study, reflections of interest occur between 150 and 220 ms. NMO correction reduces their frequency by nearly 10% (Figure 4). This is an undesirable result if quantitative analysis of derived frequency attributes is required.

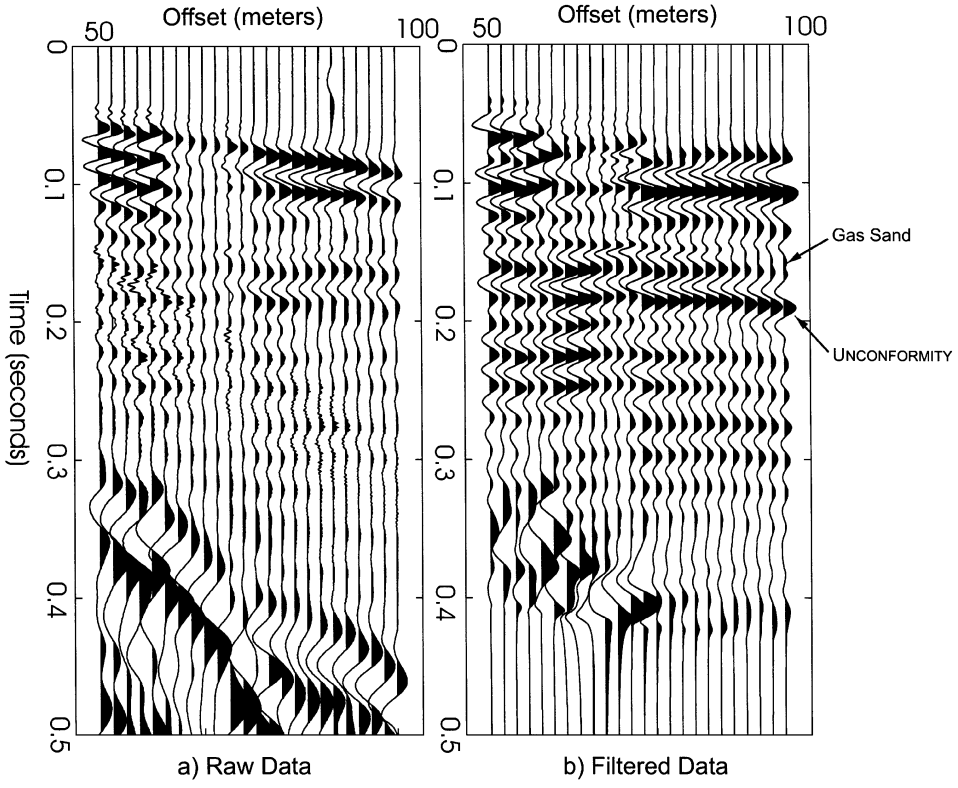

FIG. 3. (a) Typical raw 24-channel common shot gather, and (b) the same data after f-k filter application.

Additionally, large static time shifts as great as 18 ms are observed for the gas-sand event (Figure 5a) despite there being no appreciable change in the gas-sand depth across the 211-m CMP profile coverage. Consequently, substantial static time shift corrections are necessary.

Interest here focuses on detecting changes in the seismic response due to steaming of the oil sands while retaining as much of the information content of the signal as possible. NMO correction distorts the spectrum of the data and was avoided. However, the signal enhancing qualities of common midpoint trace stacking are still desirable. I reiterate that (1) the ubiquitous gas-sand event provides a convenient above-reservoir reference (Figure 5a), (2) there is very little differential moveout (<2.1 ms) between the gas-sand and unconformity events across the narrow aperture of the array (Figure 3), and (3) large static corrections are required in any processing stream (Figure 5a). Consequently, instead of carrying out the NMO correction, the peak of the gas-sand event was shifted to an arbitrary traveltime of 170 ms. An alternative procedure could be to apply a static shift of the trace based on the NMO correction for a single normal incidence time. This could then be followed by a residual static correction to properly align the reference horizon. This flattening procedure was carried out manually within common offset gathers (Figure 5b) prior to resorting the traces into CMP gathers prior to stacking. I refer to this process as shift-stacking. The final processing step consists of normalizing the shift-stack traces with respect to the peak amplitude of the gas-sand event.

Obviously, in dispensing with the NMO correction, the shift-stack data can remain valid only over a limited window centered on the gas-sand event, and it is important to evaluate potential errors. The subreservoir unconformity event was modeled simply by convolving a 50-Hz Ricker wavelet with a series of 11 traces representing the traveltimes to the unconformity over the range of offsets in the field experiment. These were then collapsed to both a single normal incidence NMO-stacked trace and a shift-stacked trace. The amplitude spectra of the shift-stack remains nearly identical to that of the input Ricker wavelet (Figure 6). The small differences result from the differential moveout between the reference gas-sand and the unconformity events. In contrast, the shape of the amplitude spectrum of the NMO stack trace, as anticipated, is moved to lower frequencies. Although the spectral distortion introduced appears small, it could profoundly influence estimates

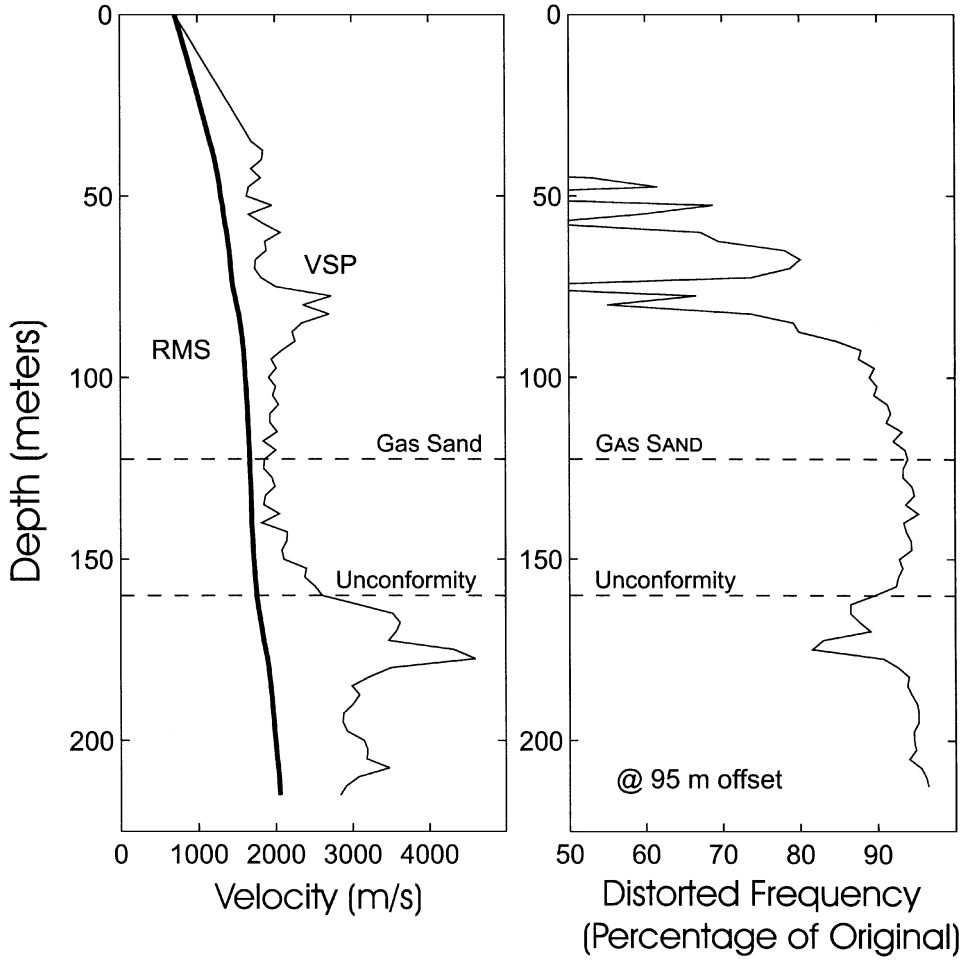

FIG. 4. Left panel: VSP-derived interval velocities and resulting rms velocities with depth. Right panel: Frequency distortion as a percentage of the original frequency resulting from NMO time stretch with depth for the rms velocity function in the left panel.

of attenuation as carried out, for example, with spectral ratio techniques.

SHIFT-STACK PROFILE ATTRIBUTES

The final shift-stack profile (Figure 7a) is shown in false colors, as this best displays lateral changes. The flattened gas-sand event, the peak amplitude of which is used in providing the prestack normalization factor for each trace, is obvious as the uniform red band at 170 ms. It is worth noting that no time-dependent gains nor any deconvolution have been applied. The data retain as much of their original character as possible, including source-point to source-point inconsistencies.

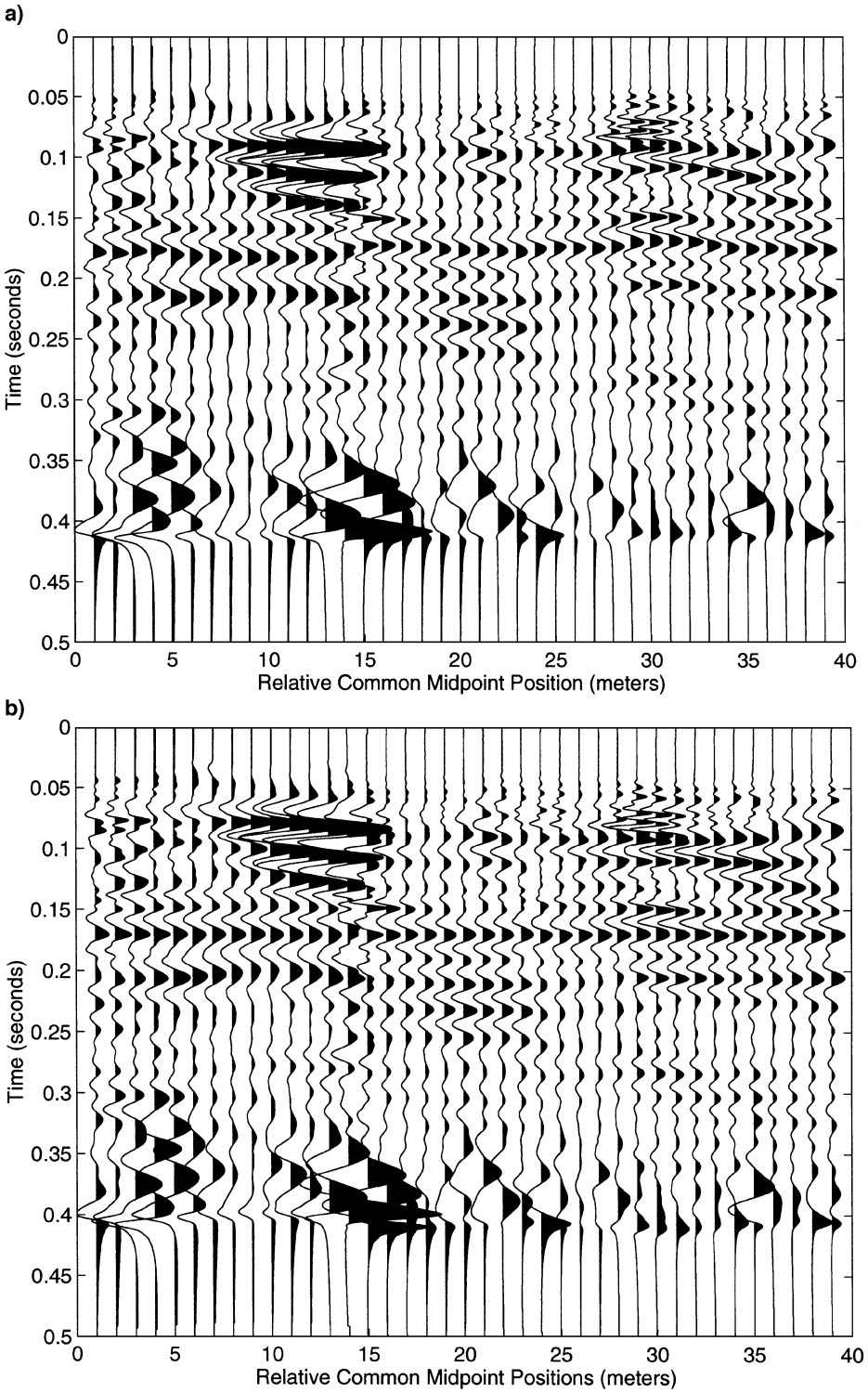

FIG. 5. (a) First 40 filtered traces of the 66-m common offset gather, common midpoint spacing of 1 m, and (b) Traces in (a) with peak of continuous gas-sand event shifted to 170 ms.

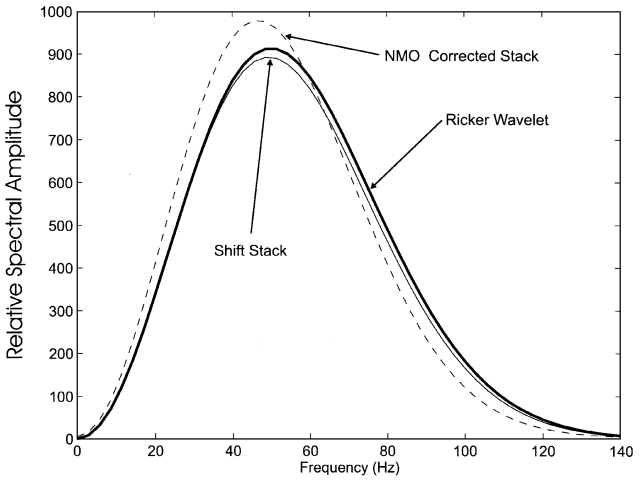

FIG. 6. Relative spectral amplitudes versus frequency of a reference 50-Hz Ricker wavelet compared to a conventional NMO-stacked trace and a shift-stack trace for the unconformity event.

The utility of stacking the data is seen at the low fold ends of the profile where the traces are of noticeably lower quality. In the vicinity of the three horizontal wells, two observations are immediately apparent: (1) the unconformity event is stronger (i.e., a bright spot) and (2) the number of cycles between the gas-sand and the unconformity changes. Below, quantitative attributes are extracted from this data set but, essentially, they derive from these two features.

The plot of the peak amplitude of the unconformity relative to that of the gas-sand (Figure 8a) changes by as much as 600%. The event is strongest in the vicinity of the horizontal wellbores.

An amplitude envelope profile (Taner et al., 1979) highlights the stronger reflections in the vicinity of the horizontal wells (Figure 7b). This attribute is a measure of the total energy within the signal at any given time (i.e., the strength of the reflection). In particular, the greatest returned energy is seen near the wells and at times of approximately 200 ms. This reinforces the observations of Figure 8a, but may not provide much in the way of additional information.

The corresponding instantaneous frequency profile (Taner et al., 1979) is more complex, displaying abrupt lateral changes

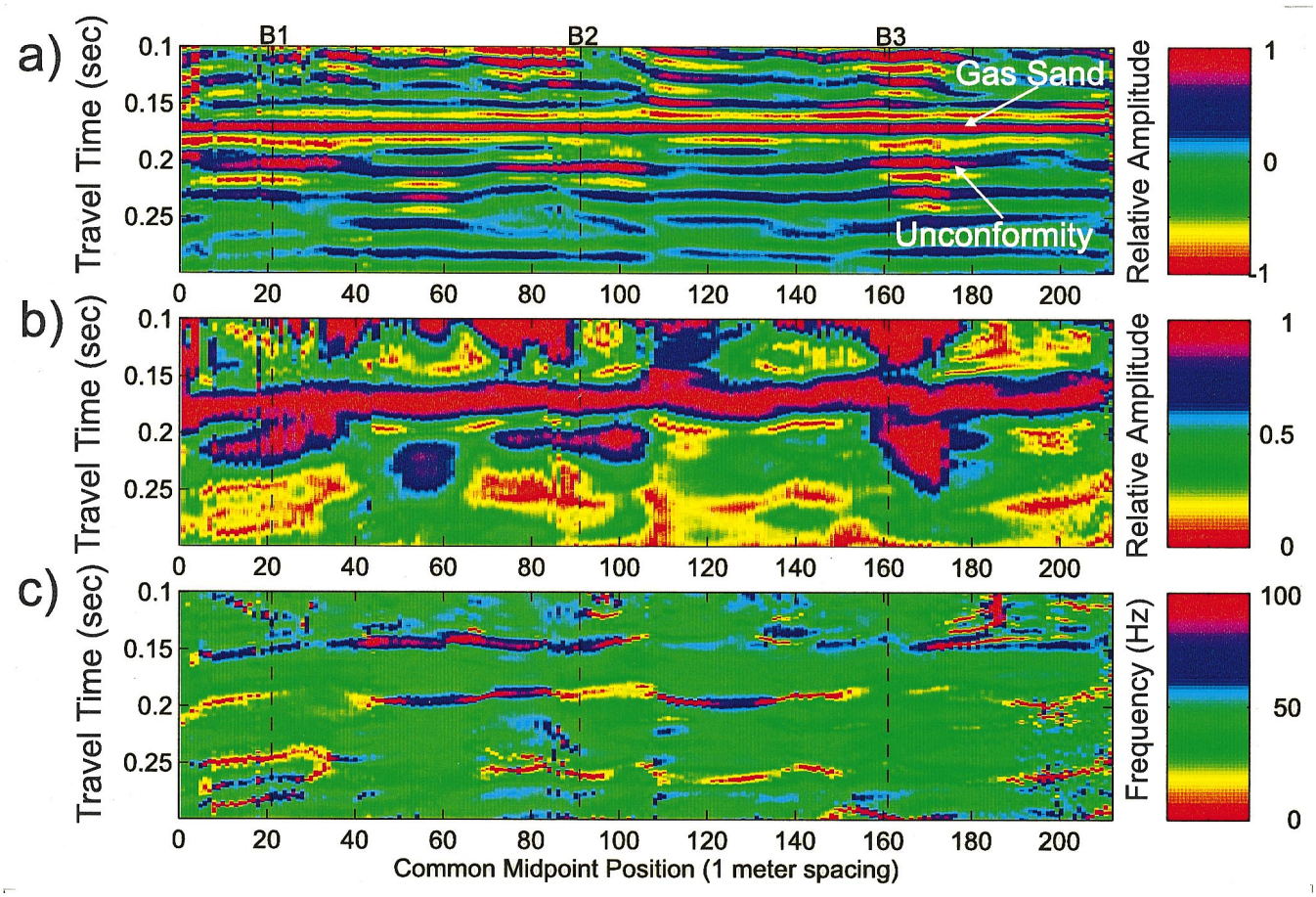

FIG. 7. (a) Shift-stack profile created by stacking of traces flattened in common offset gathers. Amplitudes normalized to the peak of the gas-sand event at 170 ms. Gas-sand and unconformity events are indicated. B1, B2, and B3 indicate the CMP positions at which horizontal wells are expected to intersect the plane of the section. (b) Amplitude envelope section of data in (a) normalized to peak energy within time window from 150 to 175 ms. (c) Instantaneous frequency section of data in (a).

(Figure 7c). The portions of this signal deriving from the gas-sand event have high instantaneous frequency and are generally continuous across the profile. The instantaneous frequency related to the unconformity near 200 ms (Figure 7c), however, varies rapidly. Near the wells, its instantaneous frequency is low (20-40 Hz). In the interwell regions (CMPs 47-84 and CMPs 109-135), this frequency is substantially greater (>80 Hz). Essentially, these high and low instantaneous frequencies indicate changes in the number of cycles seen between 150 and 250 ms in Figure 7a. The average instantaneous frequencies over 20-ms windows centered at 150 and 200 ms are plotted versus CMP position in Figure 8b. The average instantaneous frequencies for the uppermost window associated with the above-reservoir arrivals has a complex character which does not correlate with the well positions. In contrast, the instantaneous frequencies for the lower window, which includes the unconformity event, changed abruptly, being substantially lower in the vicinity of the wells.

The peak frequency of the power spectral density was calculated over a short time window (Figure 8c) to provide an additional frequency attribute. This is the spectral frequency of the greatest amplitude of the power spectrum calculated over the time window from 160 to 250 ms in each trace of Figure 7a. The power spectrum was estimated using Welch's averaged periodogram method. This window includes gas-sand and unconformity events. This peak frequency correlates well with the well positions: the frequency changes abruptly and is low (30–35 Hz) in the vicinity of the wells and noticeably higher (55–60 Hz) at interwell positions.

DISCUSSION

The shift-stack (Figure 7a) and its derivative attribute maps all indicate that the seismic character changes near the injection wells. Unfortunately, there exist no data acquired prior to steaming of the reservoir against which an adequate comparison can be made. It is possible, but unlikely, that these changes result only from variations in the geological structure existing prior to any heating of the reservoir. A reconnaissance survey acquired in the mid-1980s, prior to injection of heated fluids, does indicate the possible existence of the weaker oil sand arrival, but otherwise it is too heavily processed and of too low a lateral spacing for quantitative comparisons. Alternatively, at the time of this survey, some minor amounts of interwell disruption were observed in temperature logs. Consequently, it is impossible to unequivocally state that the observed lateral variations do not result solely from changes in the geology. However, the fact that the changes correlate closely with horizontal well positions suggests the larger disruptions of the reservoir introduced by heating and production are easily detected.

The simple modeling (Figure 2) suggested that the introduction of steam delays the traveltime and increases the reflection strength of the unconformity event, but does not change the gas-sand event. This is not what is observed (Figure 7a). The "bright spots" observed are consistent with the predictions. However, over the horizontal wellbores, the unconformity event arrives much sooner after the gas-sand event than in the colder, less disturbed regions. This indicates the modeling of Figure 2 is probably overly simplistic. One possibility is that the earlier apparent arrival time results from interference tuning

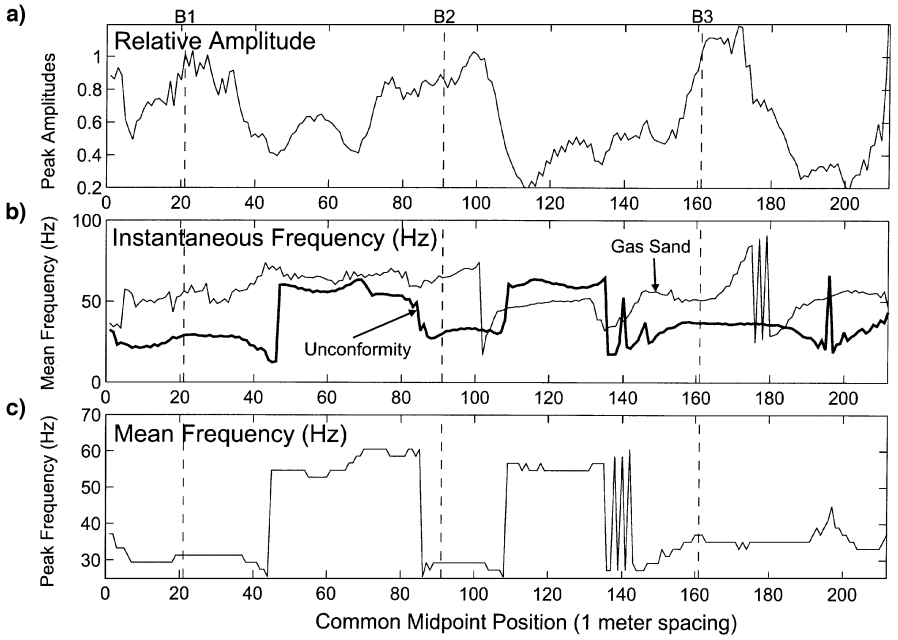

FIG. 8. (a) Relative peak positive amplitude extracted from data in Figure 7a between the unconformity and gas-sand events versus CMP position. Vertical lines indicate CMP positions at which horizontal wells B1, B2, and B3 intersect the section. (b) Averaged instantaneous frequency over 20-ms windows from Figure 7c centered on 150 ms (heavy line) and 200 ms (light line) above and below the reservoir, respectively. (c) Frequency of peak amplitude of short-time power spectra calculated over time window from 160 to 250 ms versus CMP position.

between the true unconformity reflection and a new, immediately overlying event resulting from increased pore pressures and temperatures during steaming. Another possible explanation for this discrepancy is that it may fail to adequately take into account the influence of vertical gradients of temperature and pressure on velocity. Assessing the points at which gasses exsolve from or long chain hydrocarbons melt within the complex heavy oils (Wang and Nur, 1988), both known to strongly affect the material velocity, should be employed in future modeling. However, more effective modeling is hindered by a lack of knowledge of the spatial variability of the physical properties within the reservoir.

Within a given common midpoint gather, there were no observable changes in the reflected amplitudes of the gas-sand or the unconformity events with offset [i.e. amplitude variation with offset (AVO) effect]. This is not surprising, as the contaminating shallow refractions and surface waves allow acquisition of usable data only over a small range of offsets. As a result, the angles of the rays incident on the gas-sand vary by less than 15°. Further, the dimensions of the steam zones are sufficiently small that the reflections are not scattered from a simple planar interface, making an AVO interpretation difficult.

It is interesting to note the apparent low-frequency behavior of the unconformity event near the horizontal wellbores (Figures 7c and 8c). This may be related to the "low-frequency shadows" for events returning from lithologies below gas and oil reservoirs first mentioned by Taner et al. (1979). They suggested that these phenomena might result from either increased intrinsic attenuation within the reservoir or from incorrect stacking of CMP traces due to inappropriate stacking velocities. The latter does not apply to the narrow aperture shift-stack data of Figure 8. Changes in the attenuation of the material are possibly influential here. However, the discrepant unconformity traveltimes suggest the low-frequency shadow results from tuning interference (Dilay and Eastwood, 1995).

Although perhaps obvious, changes in intrinsic material properties in effect change the geologic structure. Interpretators of seismic attributes should keep this in mind. For example, a rock physicist might be tempted to ascribe the diminished frequency content of the unconformity reflector to increased intrinsic attenuation within the reservoir. However, an alternate explanation is that the analogous changes in the overall geologic structure produce interference tuning of a new laterally discontinuous event with the unconformity reflection. In principle, deconvolution might aid in a separation of these events. In practice, shallow data, which is also highly contaminated with other undesirable arrivals, makes accurate deconvolution difficult. This is further complicated by the fact that the input wavelet is not stationary because of the rapid loss of high-frequency components.

Keeping in mind that the CMP spacing is only 1 m, the magnitudes of the attributes can vary rapidly along the profile. Indeed, in Figures 7c and 8b, the frequency attributes are discontinuous. In contrast, first Fresnel zone estimates of the lateral spatial resolution (e.g., Fowler, 1990) are would suggest that such small lateral features should not be detected. For example, given a characteristic velocity of 2400 m/s and a predominant signal frequency of 50 Hz (wavelength $\lambda = 48$ m) to the unconformity reflector at a depth of $d = 160$ m, the Fresnel zone width w given by

$$w^2 = 2d\lambda + \frac{\lambda^2}{4} \qquad (3)$$

is 126 m. Features smaller than w cannot be resolved according to this rule-of-thumb theoretical estimate. This distance is greater than the separation between the well pairs. Clearly, this estimate greatly exceeds the variations seen in the seismic signals in the present closely spaced acquisition.

The reason for this discrepancy is not yet known. One possible explanation is that equation (3) fails to account for frequency components larger than the predominant frequency of the signal. Such a reason provides further motivation for the shift-stack procedure because it does not lower the frequency due to NMO stretch. Equation (3) further assumes that energy is scattered uniformly from every point within the first Fresnel disk on the surface of the reflector. This may not be realistic; instead, one might expect that the intensity of scattering should decline as the scattered raypath diverges from the central raypath directly linking the source and receiver (Clay, 1989). Those points closer to the edge of the Fresnel disk contribute correspondingly less energy to the overall signal. A final preferred explanation is that regardless of resolution limits, the wavefield is different at every point of arrival on the surface. Consequently, each receiver point records a slightly different wavefield.

CONCLUSIONS

In this paper, an approach referred to as a shift-stack was used to process a closely spaced reflection profile acquired over a shallow heated heavy oil reservoir. The goal of this study was not to create a highly resolved seismic profile of the geologic structure but to retain as much of the original character of the waveforms as possible. Standard NMO processing can be used, but at the cost of distorting the amplitude spectra of the shallow reflections. The shift-stack data remain valid only over a certain time window and for a small aperture array.

Despite first Fresnel zone width estimates of spatial resolution which are large relative to the distance between well pairs, much smaller features are detected in the 1-m spacing CMP profile. Both amplitude and frequency attributes extracted from the final profile show considerable variation which correlates with the positions of the horizontal wellbores. Specifically, increased reflection amplitudes (bright spots) and diminished apparent frequencies coincide with these wellbore positions.

At this point, the results should only be taken at their empirical face value in that definite and large changes in magnitudes of the attributes correlate with the known positions of the three horizontal wells. This alone is of value in seismic monitoring. Although a detailed interpretation of the data is a next step, the results developed here are useful in the interpretation of surveys acquired as part of a 3-D time-lapse, permanent array experiment. Continuing work includes more sophisticated modeling of anticipated responses and a repeat survey to assess time-dependent changes in the reservoir. In-situ measurements of the material velocities using repeated VSP surveys would also allow a more thorough interpretation of the present observations.

The shift-stack procedure should be useful in environmental and geotechnical seismic applications. Typically, the underlying geology is well known, but the unwanted interference of the surface and direct arrivals degrades the seismic data quality. A suitable reference may be provided by a sharp unconformity at the bottom of a deep weathered layer or from a deep water table. Whether changes in the subsurface physical properties caused by, for example, contamination of an acquifer by

hydrocarbons is detectable with the present attribute analysis is unknown.

Although standard seismic processing procedures such as NMO correction, deconvolution, and migration have been enormously successful in the context of exploration and will continue to be of value in production-based geophysics, their use might either mask, average, or otherwise distort the original character of the signal. New processing and acquisition methodologies more akin to those employed in the nondestructive evaluation community (Bray and Stanley, 1997) may be required if attributes are to be quantitatively employed in time-lapse seismic monitoring.

ACKNOWLEDGMENTS

J. Haverstock, R. Hunt, Y. Li, E. Molz, L. Tober, and the personnel at the Alberta Energy Underground Test Facility managed by Gibson Petroleum aided the field acquisition. C. Bruins and J. Haverstock organized the data. D. Lawton generously allowed use of his seismic source. M. Burianyk, V. Wherle, and A. Schindler provided thoughtful reviews. The suggestions of the associate editor and reviewers T. Pratt and D. Johnson are greatly appreciated. This work was made possible under contracts with Alberta Energy under the former Alberta Oil Sand Technology and Research Authority and by grants from Imperial Oil and NSERC. I also acknowledge the A. VonHumboldt Foundation and Geophysikalisches Institut at the University of Karlsruhe, Germany, for support in the preparation of this manuscript.

REFERENCES

Ali, S. M., and Thomas, S., 1996, The promise and problems of enhanced oil recovery methods: J. Can. Petr. Tech., **35**, 57–63.

Batzle, M., and Wang, Z., 1992, Seismic properties of pore fluids: Geophysics, **57**, 1396–1408.

Bray, D. E., and Stanley, R. K., 1997, Non destructive evaluation; a tool in design, manufacturing, and service: CRC Press.

Butler, R., 1994, Steam-assisted gravity drainage: Concept, development, performance, and future: J. Can. Petr. Tech., **33**, No. 2, 44–50.

Chow, L., and Butler, R. M., 1996, Numerical simulation of the steam-assisted gravity drainage process (SAGD): J. Can. Pet. Tech., **35**, No. 6, 55–62.

Christensen, N. I., and Wang, H. F., 1985, The influence of pore pressure and confining pressure on the dynamic elastic properties of Berea sandstone: Geophysics, **50**, 207–213.

Clark, V. A., 1992, The effect of oil under in-situ conditions on the seismic properties of rocks: Geophysics, **57**, 894–901.

Clay, C. S., 1989, Elementary exploration seismology: Prentice-Hall, Inc.

Dilay, A., and Eastwood, J., 1995, Spectral analysis applied to seismic monitoring of thermal recovery: The Leading Edge, **14**, 1117–1122.

Domenico, S. N., 1977, Elastic properties of unconsolidated porous sand reservoirs: Geophysics, **42**, 1339–1368.

Eastwood, J., 1993, Temperature-dependent propagation of *P*- and *S*-waves in Cold Lake oil sands: Comparison of theory and experiment: Geophysics, **58**, 863–872.

Eastwood, J., Lebel, P., Dilay, A., and Blakeslee, S., 1994, Seismic monitoring of steam-based recovery of bitumen: The Leading Edge, **13**, 242–251.

Fowler, C. M. R., 1990, The Solid earth: Cambridge Univ. Press.

Hickey, C. J., Eastwood, J. E., and Spanos, T. J. T., 1991, Seismic wave propagation in oil sands: AOSTRA J. Res., 7, 67–81.

Hunter, J. A., Pullan, S. E., Burns, R. A., Gagne, R. M., and Good, R. L. O., 1984, Shallow seismic reflection mapping of the overburden-bedrock interface with the engineering seismograph—Some simple techniques: Geophysics, **49**, 1381–1385.

Kalantzis, F., Kanasewich, E., Dai, N., Kostyukevich, A., and Udey, N., 1993, Imaging of reflection seismic wavefields in thermally enhanced oil recovery projects: 63rd Ann. Internat. Mtg., Soc. Expl. Geophys., Expanded Abstracts, 335–338.

Kebaili, A., and Schmitt, D. R., 1996, Velocity anisotropy observed in wellbore seismic arrivals: Combined effects of intrinsic properties and layering?: Geophysics, **61**, 12–20.

Knapp, R. W., and Steeples, D. W., 1986, High resolution common-depth-point reflection profiling: Field acquisition parameter design: Geophysics, **51**, 283–294.

Lumley, D. E., 1995, 4-D seismic monitoring of an active steamflood: 65th Ann. Internat. Mtg., Soc. Expl. Geophys., Expanded Abstracts, 203–206.

Macrides, C. G., Kanasewich, E. R., and Bharatha, S., 1988, Multiborehole seismic imaging in steam injection heavy oil recovery projects: Geophysics, **53**, 65–75.

Mathisen, M. E., Vasiliou, A. A., Cunningham, P., Shaw, J., Justice, J. H., and Guinzy, N. J., 1995, Time-lapse crosswell seismic tomogram interpretation: Implications for heavy oil reservoir characterization, thermal recovery process monitoring, and tomographic imaging technology: Geophysics, **60**, 631–650.

Miller, R. D., 1992, Normal moveout stretch mute on shallow-reflection data: Geophysics, **57**, 1502–1507.

Nur, A., 1987, Seismic rock properties for reservoir descriptions and monitoring, *in* Nolet, G., Ed., Seismic tomography: D. Reidel Publ. Co., 203–237.

Paulsson, B. N. P., Meredith, J. A., Wang, Z., and Fairborn, J. W., 1994, The Steepbank crosswell seismic project: Reservoir definition and evaluation of steamflood technology in Alberta tar sands: The Leading Edge, **13**, 737–747.

Pullan, S. E., and Hunter, J. A., 1985, Seismic model studies of the overburden-bedrock reflection: Geophysics, **50**, 1684–1688.

Pullin, N., Matthews, L., and Hirsche, K., 1987, Techniques applied to obtain very high resolution 3-D seismic imaging at an Athabasca tar sands thermal pilot: The Leading Edge, **6**, 10–15.

Siewert, A. W., 1994, 3D seismic monitoring of steam stimulation processes at the iron river heavy oil pilots, Cold Lake, Alberta: Presented at the VII Venezuelan Geophysical Congress.

Steeples, D. W., and Miller, R. D., 1990, Seismic-reflection methods applied to engineering, environmental, and groundwater problems, *in* Ward, S., Ed., Geotechnical and environmental geophysics: Review and tutorial, 1: Soc. Explor. Geophys., 1–30.

Taner, M. T., Koehler, F., and Sheriff, R. E., 1979, Complex seismic trace analysis: Geophysics, **44**, 1041–1063.

Timur, A., 1977, Temperature dependence of compressional and shear wave velocities in rocks: Geophysics, **42**, 950–956.

Treitel, S., and Robinson, E. A., 1966, Seismic wave propagation in layered media in terms of communication theory: Geophysics, **31**, 17–32.

Wang, Z. and Nur, A., 1988, Effect of temperature on wave velocities in sands and sandstones with heavy hydrocarbons: SPE Res. Eng., **3**, 158–164.

———1990, Dispersion analysis of acoustic velocities in rocks: J. Acoust. Soc. Am., **87**, 2384–2395.

Wrightman, D., Rottenfusser, B., Kramers, J., and Harrison, R., 1989, Geology of the Alberta oil sands deposits, *in* Hepler, L. G., and Hsi, C., Eds., AOSTRA, technical handbook on oil sands, bitumens, and heavy oils: Alberta Oil Sands Technology Research Authority Technical Publication Series **6**, 3–9.

Wrightman, D. M., Attalla, M. N., Wynne, D. A., Strobl, R. S., Berhane, H., Cotterill, D. K., and Berezniuk, T., 1995, Resource characterization of the McMurray/gas-sand deposit in the Athabasca oil sands area: A synthesis, Alberta Oil Sands Technology Research Authority Technical Publication Series **10**.

Yilmaz, O., 1987, Seismic data processing: Soc. Expl. Geophys.